PROCEEDINGS OF SPIE

SPIEDigitalLibrary.org/conference-proceedings-of-spie

Dynamic higher-order Bessel-Gauss beam interference generation of rotating beams

Gabrielius Kontenis, Darius Gailevičius, Noe Jimenez, Kęstutis Staliūnas

Gabrielius Kontenis, Darius Gailevičius, Noe Jimenez, Kęstutis Staliūnas, "Dynamic higher-order Bessel-Gauss beam interference generation of rotating beams," Proc. SPIE 12131, Nanophotonics IX, 121310F (24 May 2022); doi: 10.1117/12.2621652

SPIE.

Event: SPIE Photonics Europe, 2022, Strasbourg, France

Downloaded From: https://www.spiedigitallibrary.org/conference-proceedings-of-spie on 04 Jul 2022 Terms of Use: https://www.spiedigitallibrary.org/terms-of-use

Dynamic higher-order Bessel-Gauss beam interference generation of rotating beams

Gabrielius Kontenis[a], Darius Gailevičius[a,b,*], Noé Jiménez[c], and Kęstutis Staliūnas[a,d,e]
[a]Vilnius University, Faculty of Physics, Laser Research Center, Saulėtekio Ave. 10, LT-10223, Vilnius, Lithuania
[b]Femtika LTD, Saulėtekio Ave. 15, LT-10224, Vilnius, Lithuania
[c]Instituto de Instrumentación para Imagen Molecular, Centro Mixto CSIC—Universitat Politècnica de València, 46022, València, Spain
[d]ICREA, Passeig Lluís Companys 23, 08010, Barcelona, Spain
[e]UPC, Dep. de Fisica, Rambla Sant Nebridi 22, 08222, Terrassa, Spain

Abstract

One of the key trends in laser material processing is the usage of structured laser beams. One such example is the Bessel beam with an elongated focal area and self-healing properties. Higher-order Bessel beams can be formed by axicons, spiral phase plates, or equivalently by the phase masks (holograms). In this work, a demonstration of "optical drill" beams with dynamic intensity distributions resembling the spinning mechanical drill is shown. Bessel beam mixing of two different helicities is achieved by using a Spatial Light Modulator (SLM). Both Bessel beams are formed on the same optical component – the phase mask consisting of two parts. Each part consists of spirals with different winding numbers and different periods that correspond to different step plates and axicons. Such a mask forms the stationary optical drill beam. As the beam propagates the outer and inner parts start to overlap and form the resultant interfering beam. Now, to make it a true drill, it must rotate in time. In our experiment, that is achieved by rotating one part of the combined hologram. This induces an angular offset to the interference and as a result, the orientation of the helical intensity pattern starts to rotate in time. This continuous motion gives the impression of an optical drill. With the beams dynamic properties, it could become a new tool in laser material micromachining, as a mechanical drill was to construction.

Keywords: Higher-order Bessel beams, spatial light modulator, beam interference,

1. INTRODUCTION

Discovered in the late 1980s, Jim Durnin and colleagues outlined the concept of the Bessel beam—a theoretical non-diffracting light beam with an infinite number of rings that can cover an infinite distance and requiring an infinite amount of power [1]. Those rings were the source of the Bessel beams energy and other intriguing properties as self-healing (ref). Since then, Bessel beams have found their way into many disciplines, including optical and acoustical trapping and tweezing, precision drilling of high aspect ratio holes [2,3]. Apart from zeroth-order Bessel beams, in some cases more exotic beam shapes can be beneficial. One notable example of singular beams are vortex beams, with helical wavefronts and a dark area along the optical axis in the focal area. Bessel beams with angular momentum also exhibit a central dark area but have an advantage over Laguerre-Gauss beams due to long nondiffracting region [4].

Higher-order Bessel beams can be formed by circular slits, conical lenses (axicons) [5], in addition to a spiral phase plates [6–8], or equivalently by the phase transmission masks [9–11] (holograms). Note these mechanisms have been demonstrated in acoustics, where curved surfaces can be also used [12,13]. In this work, we mix to confocal and detuned vortex beams to generate a structured beam of dynamical helical intensity [14]. If the phase mask contains a phase slip i.e. a phase change jump, dislocation of 2π, then the generated Bessel beam is helical. Phase mask in the simplest case reads: $\varphi=(\alpha 1r)/\lambda+m1\theta$, here α_1 is the radial phase slope, and $m_1=\pm 1\pm,2,\pm 3\ldots$ is the topological charge or helicity. If the topological charges of two Bessel beams are different by $|m_1-m_2|=1$ then the result is a single helix of the intensity pattern. Generally, the m-helical beam is obtained with $m=|m_1-m_2|$ (for instance, the corkscrew is a single helix, and DNA or typical mechanical drill is double-helix), by changing the signs of the topological charges the handedness (clockwise or counter-clockwise) of the intensity profile changes.

Nanophotonics IX, edited by David L. Andrews, Angus J. Bain, Jean-Michel Nunzi, Proc. of SPIE
Vol. 12131, 121310F · © 2022 SPIE · 0277-786X · doi: 10.1117/12.2621652

Downloaded From: https://www.spiedigitallibrary.org/conference-proceedings-of-spie on 04 Jul 2022
Terms of Use: https://www.spiedigitallibrary.org/terms-of-use

2. METHODOLOGY

2.1 Generation of optical drills

The idea and physical principle rely on the mixing of two vortex-Bessel beams with different helicities and different carrier frequencies [Figure 1.]. Thus, first, such beams must be generated. The initial Gaussian beams phase front is modified by a single hologram comprised of two parts. The first part of the phase describes the axicon, while the second part describes the slip phase plate with the topological charge m. The multiple-helical beams can be created by multiple phase slips $m_1 2\pi$ in axicons, or equivalently by multi-armed spirals in phase masks. The k propagation vector for a wave that propagates with phase velocity c_0, angular frequency ω, is related by:

$$k(\omega) = \frac{\omega}{c_0} = \sqrt{k_{\parallel}^2 + k_{\perp}^2} \tag{1}$$

Where $k_{\parallel}$ and $k_{\perp}$ are axial and radial components of the wave number respectively.

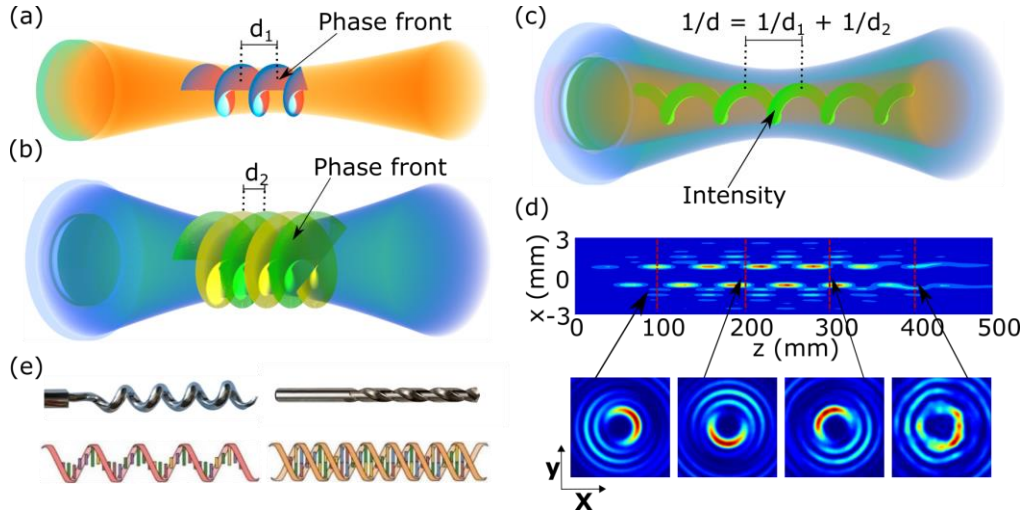


Figure 1. Generation of optical drill beams. (a) Phase-helical Bessel beam with single helicity $m_1=1$, wavefront. (b) Phase-helical Bessel beam with double helicity $m_2=2$ wavefront. (c) Optical drill bit, emerging from the interference of beams a and b, showing a helical intensity distribution. (d) Axial x-z and transverse x-y cross sections of the simulated intensity distribution. The inner beam of topological charge of $m_1=1$ is formed by axicon with the angle of 0.61°, while the outer beam as $m_1=2$ is formed by the axicon angle of 1.04°. (e) Mechanical and biological analogs with the same geometric structure to the proposed light intensity patterns, a corkscrew or RNA molecule for single helicity, and a drill bit or DNA[15].

The intensity windings occur due to the interference of two constituent Bessel beams with different longitudinal propagation wavenumbers in their overlap area. The period of winding is equal to the period the interference pattern is $d_{\parallel} = 2\pi/(k_{1,\parallel} - k_{2,\parallel})$. The longitudinal wavevector components of Bessel beams depend on their ramp or cone angle. The axial overlap area extends from the distance the outer part starts to overlap the inner and reads explicitly $D_{\parallel} = r_1(1/\alpha_1 - 1/\alpha_2)$. All this gives the number of windings along the overlap area:

$$N = \frac{D_{\parallel}}{d_{\parallel}} = \frac{r_1}{2\lambda}\frac{(\alpha_2-\alpha_1)^2(\alpha_1+\alpha_2)}{\alpha_1\alpha_2}. \tag{2}$$

Noting that the total number of spiral windings in the central disc is: $m = r_1\alpha_1/\lambda$, and introducing the definition of ratio of ramps: $\alpha = \alpha_2/\alpha_1$ we finally obtain a simple expression:

$$N = \frac{m}{2}(\alpha - 1)^2(\alpha + 1)/\alpha. \tag{3}$$

For the typical ramp ratio $\alpha \approx 2$ we conclude that the number of windings in optical screw N is equal to the number of windings of spirals in the central disc of the axicon m.

Downloaded From: https://www.spiedigitallibrary.org/conference-proceedings-of-spie on 04 Jul 2022
Terms of Use: https://www.spiedigitallibrary.org/terms-of-use

2.2 Numerical propagation

By using a Fourier split step method, a simulation of the propagation of such a beam was done and visualized in [Figure 2]. In this case the base topological charges used were $m_1 = 4$ and $m_2 = 7$ which gives us a topological charge difference of 3 and the interference results in 3 winding maxima. After the interference, the structure collapses into rings that represent the Higher order Bessel far fields.

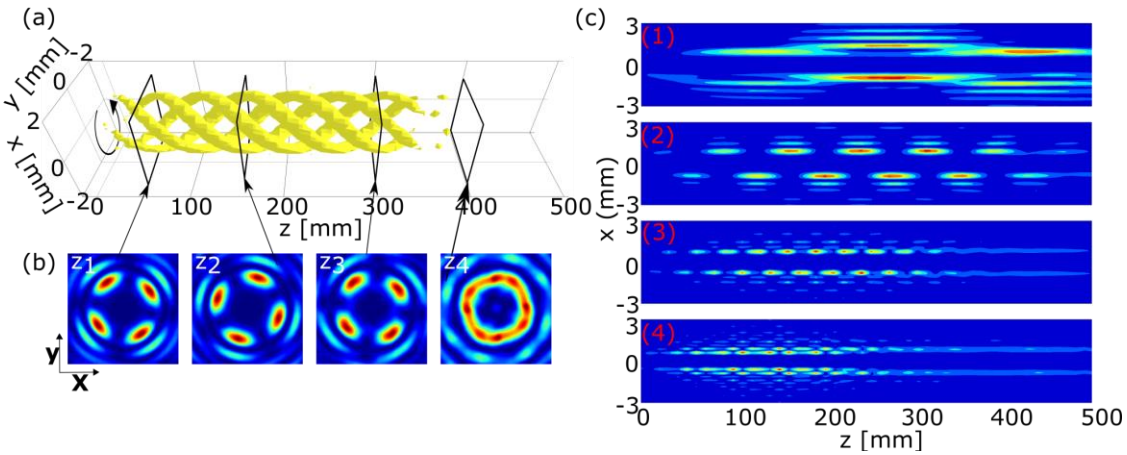


Figure 2. Numerical simulation of an optical drill. (a) 3D iso-surface model of the interference of two Bessel-Gauss beams creating the spiral intensity structure - optical drill. The figure shows a 3-arm optical drill formed by two Bessel beams of ($m_1 = 4$, $m_2 = 7$). (b) Simulated *x-y* cross-section intensity distributions at different planes. (c) Simulated slices of intensity distribution in x-z planes with different axicon angle ratios. (1) ratio of 1.1, (2) ratio of 1.4 (3) ratio of 1.8 and (4) a ratio of 2.3. When the ratio is too small (case 1), the beams propagate mostly at their own ring shapes. When the ratio is too big (case 4), the outer beam quickly overlaps with the inner beam, creating fast intensity oscillations and quickly diverges away.

There is a delicate balance between the best parameter set to obtain a stable optical drill. The most crutial being the ratio of the Bessel angles [Figure 2c]. If the angle ratio is too large the outer Bessel overlaps the inner one very rapidly and quickly diverges. The total length of the beam and it's shape becomes heavily distorted. In the worst case, the beams propagate as separate (nonoverlapping) tubes, with some distortions on the edges from partial interference.

2.3 Experimental realization

To experimentally generate such a beam a Liquid Crystal Spatial Light Modulator (SLM) was used [Figure 3a]. The entire beam was generated by a single hologram comprised of two parts [Figure 3b]. Each part generates one of the two interfering Bessel beams. This way is very flexible as it allows us to use a single input Gaussian beam, and at the output get the optical drill. In addition, the hologram has a diffraction grating added to separate the zero-diffraction order from the wanted Bessel structures. Of course, such a method has drawbacks, as the length of the drill is determined by the central spots size, and you must tune the energies of each of the Bessel in proportion to the incoming Gaussian beam to not have a dominant Bessel beam, that still creates a visible ring. Because the SLM is a dynamical element, we can induce rotation of the entire beam in time. In doing so, the apparent forward and backward motion of the entire structure appears.

Downloaded From: https://www.spiedigitallibrary.org/conference-proceedings-of-spie on 04 Jul 2022
Terms of Use: https://www.spiedigitallibrary.org/terms-of-use

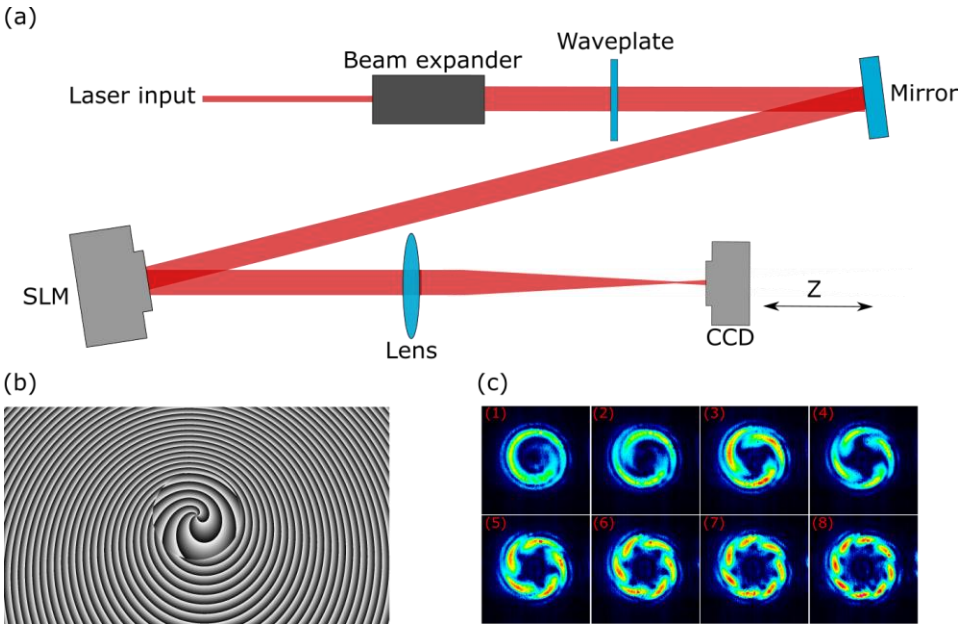


Figure 3. The optical scheme used for beam shaping with experimental holograms. a) The incoming laser beam is expanded to reduce the power density and effectively use the active SLM area. A half waveplate is used to align the laser polarization with the nematic liquid crystals of the SLM. A final focusing lens and a CCD camera for visualizing the beam. A 4F system comprised of two lenses could be used to relay the phase front from the SLM plane to the final focusing objective input pupil plane in systems. b) Phase masks reproducing the axicon combined with a spiral phase plate. Grayscale phase image computer generated holograms displayed on the SLM. Black areas correspond to a phase shift of 0, where white areas correspond to *– 2pi* central Bessel with *m = 5*, outer Bessel *m = 9*. The inner Bessel disk size is calibrated to equally divide the initial Gaussian beams energy. c) Experimental comparison of transverse intensity distribution of two interfered Bessel-Gauss beams. From (a) to (h) the outer Bessel-Gauss beam topological charge was changed from 2 to 9. The intensity distribution has the number of maxima equal to the topological charge difference of both beams. The resultant beam size remains constant.

Various XY cross sections were generated with different topological charge differences that are visible in the number of maxima (arms) of the resultant beam's intensity distribution [Figure 3c]. The diameter of the optical drill can be modified by changing the base topological charges of the interfering beams while maintaining the difference constant. In doing so, a larger central hole is formed with more stretched out intensity maxima around the center. Therefore, $m = 3$ for all cases. However, as the width of the core of the main vortices is larger for higher topological charges, the diameter of the beam grows almost linearly with increasing topological charges.

3. CONCLUSIONS

Light beams with rotating helical intensity distribution emerge as the spatiotemporal interference of high-order Bessel beams with different axicon angles, different topological charges, and different carrier frequencies. The parameters of the optical drills, i.e., its length, radius, winding period, and the order of helical structure, are highly tunable. In addition, the sense of rotation and rotation frequency of the drill can be set by adjusting the frequency detuning. A principle of generating such beams by using a single dynamic optical element has been shown. While the rotation of the SLM hologram is sufficient to demonstrate the principle, the rotation frequency must be strongly increased for technologically relevant applications, e.g., using acousto-optical devices to obtain two coherent Bessel beams of coherently different frequencies.

Like the case of stationary helical beams[16], the optical drill could become a tool for particle micromanipulation[17]. Moreover, its rotation in time can add the possibility of attracting or pushing particles along the optical axis.

Downloaded From: https://www.spiedigitallibrary.org/conference-proceedings-of-spie on 04 Jul 2022
Terms of Use: https://www.spiedigitallibrary.org/terms-of-use

ACKNOWLEDGMENTS

This work has received funding from European Social Fund (project No 09.3.3- LMT-K712-17- 0016) under grant agreement with the Research Council of Lithuania (LMTLT), also from the Spanish Ministry of Science, Innovation and Universities (MICINN) under grants PID2019-109175GB-C21 and PID2019-111436RB-C22. NJ acknowledges financial support MICINN through grant "Juan de la Cierva – Incorporación" IJC2018-037897-I and Agència Valenciana de la Innovació through grant INNVA1/2020/92.

REFERENCES

[1] Durnin, J., Miceli, J. J. and Eberly, J. H., "Diffraction-free beams," Phys. Rev. Lett. **58**(15), 1499–1501 (1987).
[2] Duocastella, M. and Arnold, C. B., "Bessel and annular beams for materials processing," Laser Photonics Rev. **6**(5), 607–621 (2012).
[3] Jiménez, N., Romero-García, V., Picó, R., Cebrecos, A., Sánchez-Morcillo, V. J., Garcia-Raffi, L. M., Sánchez-Pérez, J. V. and Staliunas, K., "Acoustic Bessel-like beam formation by an axisymmetric grating," EPL (Europhysics Lett. **106**(2), 24005 (2014).
[4] Mendoza-Hernández, J., Arroyo-Carrasco, M. L., Iturbe-Castillo, M. D. and Chávez-Cerda, S., "Laguerre–Gauss beams versus Bessel beams showdown: peer comparison," Opt. Lett. **40**(16), 3739 (2015).
[5] Mcgloin, D. and Dholakia, K., "Bessel beams: Diffraction in a new light," Contemp. Phys. **46**(1), 15–28 (2005).
[6] Jiménez, N., Sánchez-Morcillo, V. J., Picó, R., Garcia-Raffi, L. M., Romero-Garcia, V. and Staliunas, K., "High-order acoustic Bessel beam generation by spiral gratings," Phys. Procedia **70**, 245–248 (2015).
[7] Jiménez, N., Picó, R., Sánchez-Morcillo, V., Romero-García, V., García-Raffi, L. M. and Staliunas, K., "Formation of high-order acoustic Bessel beams by spiral diffraction gratings," Phys. Rev. E **94**(5) (2016).
[8] Jiménez, N., Romero-García, V., García-Raffi, L. M., Camarena, F. and Staliunas, K., "Sharp acoustic vortex focusing by Fresnel-spiral zone plates," Appl. Phys. Lett. **112**(20), 204101 (2018).
[9] Durfee, C. G., Gemmer, J. and Moloney, J. V., "Phase-only shaping algorithm for Gaussian-apodized Bessel beams," Opt. Express **21**(13), 15777 (2013).
[10] Jiménez-Gambín, S., Jiménez, N. and Camarena, F., "Transcranial Focusing of Ultrasonic Vortices by Acoustic Holograms," Phys. Rev. Appl. **14**(5), 54070 (2020).
[11] Jiménez-Gambín, S., Jiménez, N., Benlloch, J. M. and Camarena, F., "Generating Bessel beams with broad depth-of-field by using phase-only acoustic holograms," Sci. Rep. **9**(1) (2019).
[12] Jiménez, N., Ealo, J., Muelas-Hurtado, R. D., Duclos, A. and Romero-Garciá, V., "Subwavelength Acoustic Vortex Beams Using Self-Demodulation," Phys. Rev. Appl. **15**(5) (2021).
[13] Jiménez, N., Camarena, F. and Staliunas. Kestutis., "Sistema y método de generación de haces acústicos confocales de vórtice con superposición espaciotemporal," Patent No: ES2811650A1, 41 (2021).
[14] Kontenis, G., Gailevičius, D., Jiménez, N. and Staliunas, K., "Optical Drills by Dynamic High-Order Bessel Beam Mixing," Phys. Rev. Appl. **17**(3), 1–7 (2022).
[15] Aryal, S., "30 Differences between DNA and RNA (DNa vs RNA)," Microbe Notes, 2020, <https://microbenotes.com/differences-between-dna-and-rna/> (17 November 2021).
[16] Volke-Sepulveda, K., Garcés-Chávez, V., Chávez-Cerda, S., Arlt, J. and Dholakia, K., "Orbital angular momentum of a high-order Bessel light beam," J. Opt. B Quantum Semiclassical Opt. **4**(2) (2002).
[17] Simpson, S. H. and Hanna, S., "Orbital motion of optically trapped particles in Laguerre–Gaussian beams," J. Opt. Soc. Am. A **27**(9), 2061 (2010).

Downloaded From: https://www.spiedigitallibrary.org/conference-proceedings-of-spie on 04 Jul 2022
Terms of Use: https://www.spiedigitallibrary.org/terms-of-use